Nernst effect in Tl-Ba-Ca-Cu-O high-T_c superconducting thin films

S. Zeuner, W. Prettl, K.F. Renk, and H. Lengfellner
Institut für Angewandte Physik, Universität Regensburg, 93040 Regensburg, Germany.
(Received 13 July 1993)

The dynamical behavior of magnetic flux in superconducting Tl-Ba-Ca-Cu-O films has been studied using the Nernst effect. Large temperature gradients of $\sim 10^5$ K/cm and, correspondingly, large thermal forces on flux lines were obtained by pulsed laser heating of films. Due to the large thermal driving forces it was possible to observe, at temperatures well below T_c, the transition from thermally assisted flux flow to flux creep and viscous flux flow.

The transport properties of the magnetic flux structure in high-T_c superconductors have attracted much attention during the last few years. A number of groups concentrated on the investigation of current-induced flux motion (see, e.g., Refs. 1 and 2), where a transport current applied perpendicular to the magnetic field in a superconducting sample exerts a Lorentz force on the flux lines and thus leads to flux motion. Recently, in another type of experiments, thermally driven flux motion was investigated,[3–13] where the thermal force due to a temperature gradient within the superconductor causes the flux lines to move. The vortices, moving with velocity $\mathbf{v}$ generate an electric field perpendicular to the temperature gradient and the magnetic field, the Nernst field $\mathbf{E} = \mathbf{B} \times \mathbf{v}$. The dependence of the Nernst field on temperature and driving force provides information about the dynamics of flux motion and the influence of pinning. In addition, measurements of the Nernst and Ettingshausen effects in the regime of viscous flux flow were carried out by continuous heating methods to determine the transport entropy S_Φ connected with a moving vortex, for $YBa_2Cu_3O_{7-\delta}$,[5–11] Bi- (Ref. 12) and Tl- (Refs. 12 and 13) based superconductors. While these experiments work typically with small temperature gradients of ~ 10 K/cm, we report here an experiment where the temperature gradient is generated by absorption of a laser pulse at the surface of a thin film.[3,4] In contrast to continuous heating methods temperature gradients of up to 10^6 K/cm can be obtained with this technique, so that thermally driven flux motion can be studied over an extremely wide range of driving forces. This allows one for the first time to observe the transition from thermally assisted flux flow to flux creep and viscous flux flow well below T_c in Tl-Ba-Ca-Cu-O thin films.

At temperatures close to T_c or at large driving forces the flux motion will be determined by viscous flux flow. The Nernst field is then given by[14]

$$E = \frac{S_\Phi \rho_{FF}}{\Phi_0} \nabla T, \tag{1}$$

where S_Φ is the transport entropy of a vortex per unit length, ρ_{FF} the resistivity due to the motion of Abrikosov vortices, and Φ_0 the magnetic flux quantum. At lower temperatures, where the pinning of flux lines becomes effective, the vortices do not move with a constant velocity but jump between pinning sites preferably along the direction of the driving force. The Nernst field is then found using Anderson's model of thermally activated hopping[4,15,16]

$$E = 2B\nu_0 l \exp(-U_a/k_BT) \sinh\left(\frac{U_a}{k_BT} \frac{\nabla T}{(\nabla T)_c}\right) \tag{2}$$

with a critical temperature gradient $(\nabla T)_c$ defined by

$$U_a = (\nabla T)_c S_\Phi L_c r_p, \tag{3}$$

where L_c is the correlated length of a flux line, r_p the range of the pinning potential, ν_0 a characteristic attempt frequency for flux hopping, l the hopping distance and U_a the activation energy of the hopping process. For small driving forces, i.e. small temperature gradients, the hyperbolic sine in Eq. (2) can be linearized and the Nernst field is expected to be proportional to the driving force. With increasing temperature gradient the energy gain $U = \nabla T S_\Phi L_c r_p$ of a vortex moving over a distance r_p under the action of the thermal force becomes comparable to the pinning energy. The number of jumps along the force increases then drastically, leading to flux creep with an exponential dependence of E on ∇T. For $\nabla T \gtrsim (\nabla T)_c$ the influence of pinning becomes small and the viscous drag force determines the flux motion as expressed by Eq. (1).

The time-dependent temperature distribution within the sample can be described using a heat transfer model.[17] A laser pulse with energy E_p per unit area is absorbed at the film surface and heats the film within the penetration depth of the radiation being about 100 nm. The heat flow through the film is determined by the thermal diffusivity D. In rather thick films ($d \sim 1$ μm), as used in our experiment, the influence of the thermal boundary resistance connected with the film-substrate interface is small and can be neglected. The temperature gradient across the film is then given by[17]

$$\nabla T(t) = E_p \frac{2A}{Cd^2} \sum_{n\ \mathrm{odd}} \exp\left(-\frac{n^2\pi^2}{4d^2} Dt\right), \tag{4}$$

where A is the absorptivity, C the specific heat per unit volume, d the thickness, and D the thermal diffusivity of the film. Only the first few terms of the sum in Eq. (4)

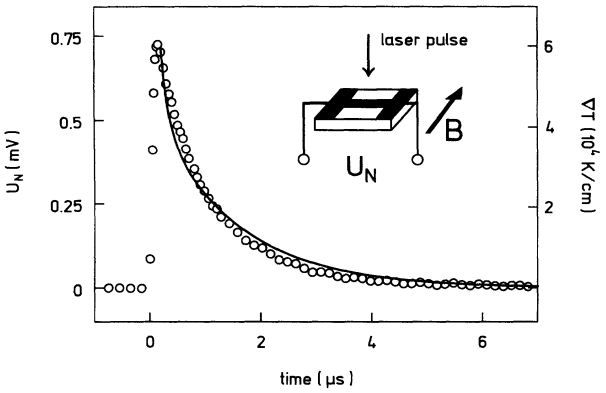

FIG. 1. Nernst signal at T= 70 K (circles, left scale) and calculated temperature gradient (line, right scale). Inset shows experimental arrangement.

give rise to a significant contribution. For sample temperature T and a fixed time t, e.g., the time where the maximum of the Nernst voltage is observed, the temperature gradient is proportional to the laser fluence. Then Eqs. (1) and (2) can be rewritten to give the Nernst field as a function of the laser fluence using $\nabla T = \text{const} \times E_p$. The different regimes of flux motion are then expected to be observed at small (TAFF), intermediate (flux creep), or large (flux flow) values of E_p.

The measurements were carried out on a 1 μm thick polycrystalline Tl-Ba-Ca-Cu-O film with $T_c \simeq 110$ K, deposited on a (100) MgO substrate by laser ablation.[18] X-ray analysis showed the film to consist mainly of the (2223) phase with smaller amounts of the (2212) phase. The film was patterned into a 200 μm wide stripe and Au pads on both ends provided contacts of low resistance. The sample was placed in a temperature variable optical cryostat where magnetic fields up to 5 T could be applied parallel to the film surface. The film was heated by radiation pulses from an atmospheric pressure CO_2 laser (pulse duration $\sim$ 80 ns, wavelength $\approx$ 10 μm). The resulting Nernst voltage was amplified and recorded with a storage oscilloscope. The observed signals rise as fast as the laser pulse and decay in several μs, due to the decay of the temperature gradient across the sample by heat diffusion. A typical Nernst signal recorded at sample temperature T = 70 K is shown in Fig. 1. Also shown is the time-dependent temperature gradient calculated with Eq. (4), using $D = 3 \times 10^{-3}\,\text{cm}^2/\text{s}$, a value obtained from bolometric response measurements with the same sample.[17] The overall temperature increase of the film is of the order of 1 K. Figure 1 clearly demonstrates that the time evolution of the Nernst voltage is governed by the decaying temperature gradient.

Figure 2 shows the peak Nernst signal for B = 5 T at temperatures T = 100 K, 70 K, and 55 K for input laser fluences ranging from 2 μJ/cm^2 to 5 mJ/cm^2. For high driving forces the Nernst voltage is proportional to the laser fluence at all three temperatures, as expected in the regime of viscous flux flow [Fig. 2(a)]. At 100 K, close to T_c, pinning is insignificant and the flux motion is viscous even at the smallest fluences used in our experiment [100 K data in Figs. 2(a) and 2(b)] in accordance to continuous heating methods.

At lower temperatures we observe a deviation from the linear flux flow regime for small driving forces as shown in Fig. 2(a). There, flux pinning has to be taken into account, so that the flux motion must be described in terms of thermally assisted flux flow [Eq. (2)]. In Fig. 2(b) the low-fluence part of the data is shown on an extended scale. The solid curves represent a fit of Eq. (2) to the 70 K and 55 K data in the form $U_N = a \cdot \sinh(b \cdot E_p)$ with $a\,(70\,\text{K}) = 50\ \mu\text{V}$, $b\,(70\,\text{K}) = 5\,\text{cm}^2/\text{mJ}$, $a\,(55\,\text{K}) = 15\ \mu\text{V}$, and $b\,(55\,\text{K}) = 3\,\text{cm}^2/\text{mJ}$. Using Eq. (4) and measured values for the specific heat[19] and the diffusivity[17] of Tl-Ba-Ca-Cu-O, we find for the temperature gradient achievable by laser heating $\nabla T = f(T)\,E_p$ with $f(70\,\text{K}) = 10^6\ \text{K m/J}$ and $f(55\,\text{K}) = 1.25 \times 10^6\ \text{K m/J}$. From Eq. (2) we obtain for the critical temperature gradient $(\nabla T)_c = \frac{U_a}{k_B T}\frac{f(T)}{b}$. With an activation energy $U_a \simeq 500$ K (see below) we find temperature gradients $(\nabla T)_c = 1.5 \times 10^5\,\text{K/cm}$ and $4 \times 10^5\,\text{K/cm}$ at sample temperatures T = 70 K and 55 K, respectively, and for the product of attempt frequency and hopping length $\nu_0 l \simeq 500$ cm/s. The large values of $(\nabla T)_c$ clearly demonstrate that by the method of transient laser heating all three regimes of flux motion (TAFF, flux creep, viscous flux flow) can be investigated at lower temperatures. TAFF, where the Nernst field is proportional to the driving force, is observed at small laser fluences. This region is followed by flux creep, characterized by an exponential increase of

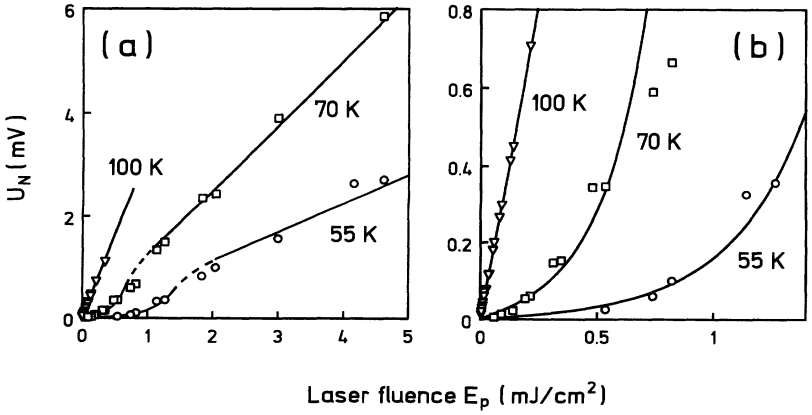

FIG. 2. Peak Nernst voltage vs input laser fluence at T= 100 K (triangles), 70 K (squares) and 55 K (circles). 2(b) shows the low-fluence part of (a) on an extended scale. Also shown are fits to the viscous flux flow regime (solid lines) and to the flux creep and TAFF regime (solid curves). The broken curves indicate an intermediate region between flux creep and viscous flux flow.

the Nernst field (solid curves in Fig. 2). An intermediate region [indicated by broken curves in Fig. 2(a)] shows the crossover from thermally activated to viscous flux flow observed at high laser fluences [solid lines in Fig. 2(a)]. The different dynamical behavior of TAFF, creep and viscous flow becomes increasingly pronounced with decreasing temperature[20] and vanishes if the temperature approaches T_c.

The transport entropy S_Φ can be estimated from the slope of the curves U_N versus E_p in the flux flow regime using Eqs. (1) and (4). The temperature gradient is calculated for the time of the peak signal (≈ 0.2 μs after absorption of the laser pulse). Assuming that the resistivity of the sample ρ is due to flux motion, i.e., $\rho_{FF} = \rho$ in Eq. (1) we obtain $S_\Phi \simeq 10^{-16}$ J/K m at $T = 70$ K, and half that value at 100 K and 55 K. These values compare well with measurements of Dascoulidou *et al.*[12] who found $S_\Phi \sim 0.2 - 1 \times 10^{-16}$ J/K m for Tl 2:2:2:3 polycrystals at $B = 5$ T and $T = 75$ K–120 K. Logvenov, Hartmann, and Huebener[13] reported $S_\Phi \simeq 3 \times 10^{-16}$ J/K m for a Tl 2:2:1:2 single crystal at $B = 1$ T and $T = 80$ K. The values reported for YBCO (Refs. 5–11) are usually about a factor of 10 larger but differ by 2 orders of magnitude depending on the microscopic structure of the sample.

The activation energy for flux hopping U_a can be estimated from the temperature dependence of the Nernst voltage. We recorded the Nernst signal at a small, constant laser fluence where the flux motion is in the TAFF regime (inset of Fig. 3). Equation (2) can then be rewritten in the form

$$\ln(U_N T) = c - \frac{U_a}{k_B T}, \tag{5}$$

where c is only weakly dependent on temperature. By replotting the Nernst voltage times T on a logarithmic scale versus inverse temperature the activation energy U_a is extracted from the slope of the curve. Figure 3 shows that the temperature interval 50–90 K can be described by a single activation energy $U_a \simeq 500$ K which indicates one dominant pinning mechanism. Similar values are reported by Pankert *et al.*[21] who found for $Tl_2Ba_2Ca_2Cu_3O_x$ ceramics an activation energy $U_a = 480$ K at 5 T using a magnetoacoustic method, and Dascoulidou *et al.*[12] who found $U_a \simeq 500$ K at 5 T for Tl 2:2:2:3 polycrystals evaluating the temperature dependence of the thermopower. The values reported for the Bi compounds are of the same order of magnitude.[2,21] The small and only weakly temperature-dependent activation energies seem to be a common feature of these very anisotropic superconductors.[22]

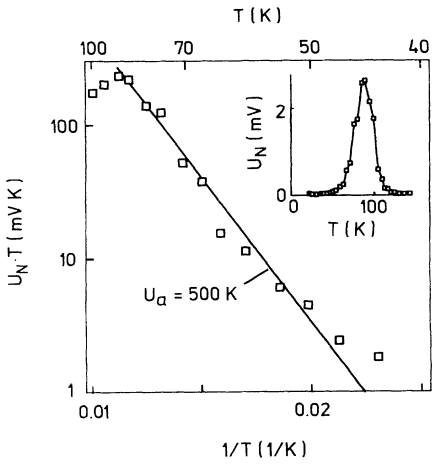

FIG. 3. Peak Nernst voltage times absolute temperature vs inverse temperature for a constant laser fluence of $E_p = 0.8\,\mathrm{mJ/cm^2}$. The line corresponds to an activation energy of 500 K. The inset shows the Nernst signal vs temperature on a linear scale.

In conclusion, we investigated the Nernst effect in the mixed state of Tl-based high-T_c thin films, where a temperature gradient between film surface and bottom is generated by pulsed laser heating. We demonstrated for the first time the three regimes of flux motion. At small temperature gradients, i.e., small driving forces, we observe thermally activated flux flow. Increasing temperature gradients lead to flux creep, once the thermal force energy is of the order of the pinning energy. High driving forces render pinning insignificant and viscous flux flow is observed. At temperatures considerably below T_c, where the different regimes can be separated clearly, temperature gradients of the order of 10^5 K/cm are necessary to observe all three regimes. The transport parameters extracted from the data are in good agreement with results obtained by different methods.

This work was supported by the Deutsche Forschungsgemeinschaft (H.L.), the Bayerische Forschungsstiftung through the Forschungsverbund Hochtemperatur-Supraleiter (FORSUPRA) (K.F.R.), and the European Communities (W.P.).

[1] T.T.M. Palstra, B. Batlogg, L.F. Schneemeyer, and J.V. Waszczak, Phys. Rev. Lett. **61**, 1662 (1988).
[2] T.T.M. Palstra, B. Batlogg, R.B. van Dover, L.F. Schneemeyer, and J.V. Waszczak, Phys. Rev. B **41**, 6621 (1990).
[3] H. Lengfellner, A. Schnellbögl, J. Betz, W. Prettl, and K.F. Renk, Phys. Rev. B **42**, 6264 (1990).
[4] H. Lengfellner and A. Schnellbögl, Physica C **174**, 373 (1991).
[5] M. Zeh, H.-C. Ri, F. Kober, R.P. Huebener, A.V. Ustinov, J. Mannhart, R. Gross, and A. Gupta, Phys. Rev. Lett. **64**, 3195 (1990).
[6] S.J. Hagen, C.J. Lobb, R.L. Greene, M.G. Forrester, and J. Talvacchio, Phys. Rev. B **42**, 6777 (1990).

[7] F. Kober, H.-C. Ri, R. Gross, D. Koelle, R.P. Huebener, and A. Gupta, Phys. Rev. B **44**, 11 951 (1991).
[8] T.T.M. Palstra, B. Batlogg, L.F. Schneemeyer, and J.V. Waszczak, Phys. Rev. Lett. **64**, 3090 (1990).
[9] M. Oussena, R. Gagnon, Y. Wang, and M. Aubin, Phys. Rev. B **46**, 528 (1992).
[10] C. Hohn, M. Galffy, A. Dascoulidou, A. Freimuth, H. Soltner, and U. Poppe, Z. Phys. B **85**, 161 (1991).
[11] R.P. Huebener, F. Kober, H.-C. Ri, K. Knorr, C.C. Tsuei, C.C. Chi, and M.R. Scheuermann, Physica C **181**, 345 (1991).
[12] A. Dascoulidou, M. Galffy, C. Hohn, N. Knauf, and A. Freimuth, Physica C **201**, 202 (1992).
[13] G.Yu. Logvenov, M. Hartmann, and R.P. Huebener, Phys. Rev. B **46**, 11 102 (1992).
[14] R.P. Huebener, *Magnetic Flux Structures in Superconductors* (Springer, Berlin 1979).
[15] P.W. Anderson, Phys. Rev. Lett. **9**, 309 (1962).
[16] R.P. Huebener, F. Kober, R. Gross, and H.-C. Ri, Physica C **185-189**, 349 (1991).
[17] S. Zeuner, H. Lengfellner, J. Betz, K.F. Renk, and W. Prettl, Appl. Phys. Lett. **61**, 973 (1992).
[18] J. Betz, A. Piehler, E.V. Pechen, and K.F. Renk, J. Appl. Phys. **71**, 2478 (1992).
[19] A. Junod, E. Eckert, G. Triscone, J. Muller, and V.Y. Lee, Physica C **162-164**, 476 (1989).
[20] E.H. Brandt, Physica C **195**, 1 (1992).
[21] J. Pankert, A. Comberg, P. Lemmens, P. Fröning, and S. Ewert, Physica C **182**, 291 (1991).
[22] T.T.M. Palstra, B. Batlogg, L.F. Schneemeyer, and J.V. Waszczak, Phys. Rev. B **43**, 3756 (1991).